THE BALTIC JOURNAL
OF ROAD AND BRIDGE ENGINEERING
2026/21(3)

ISSN 1822-427X/eISSN 1822-4288
2026 Volume 21 Issue 3: 77–102
https://doi.org/10.7250/bjrbe.2026-21.683

A REAL-TIME PEDESTRIAN-VEHICLE COLLISION RISK WARNING FRAMEWORK AT SIGNALIZED INTERSECTIONS USING TRAJECTORY PREDICTION AND DYNAMIC CONFLICT THRESHOLDS

HAOLIANG SHEN, YUQUAN MENG, YIHE HUO, YONGGANG WANG*

School of Transportation Engineering, Chang'an University, Xi'an, China

Received 31 March 2026; accepted 28 August 2026

Abstract. Pedestrian-vehicle collisions remain a critical safety concern at urban intersections, where existing risk assessment methods often rely on static conflict thresholds that lack adaptability to dynamic traffic conditions. To address this gap, this study develops a real-time pedestrian–vehicle collision risk warning framework integrating Hidden Markov Model-based vehicle trajectory prediction, an improved minimum extended time-to-collision ($ETTC_{\min}$) conflict indicator with dynamic thresholds derived via spline interpolation based on the real-time vehicle-to-pedestrian ratio, and a probabilistic conflict-based collision risk estimation model incorporating driver reaction and braking times. Validated using the SinD dataset and field data from Xi'an, the proposed method demonstrates robust trajectory prediction accuracy, earlier hazard detection compared to traditional time-to-collision metrics. By enabling adaptive, interpretable, and real-time risk warnings, this approach provides a proactive and scientifically grounded tool for enhancing pedestrian safety and supporting targeted traffic management interventions at intersections.

* Corresponding author. E-mail: wangyg@chd.edu.cn

Haoliang Shen (ORCID ID 0009-0009-5745-2677)
Yuquan Meng (ORCID ID 0009-0001-6049-5020)
Yihe Huo (ORCID ID 0009-0008-7925-4180)
Yonggang Wang (ORCID ID 0000-0002-9365-1851)

Keywords: hidden Markov models, pedestrian-vehicle collisions, road intersections, risk warning, traffic conflict technique.

Introduction

According to the World Health Organization's 2023 Global Status Report on Road Safety, road traffic crashes cause approximately 1.19 million deaths annually, 23% of which involve pedestrians (World Health Organization, 2023). In Chinese cities, approximately 30% of crashes occur at at-grade intersections (Ma et al., 2021). As pedestrians are vulnerable road users facing substantially higher fatality risks than vehicle occupants, mitigating risk during pedestrian-vehicle interactions is essential.

Research on pedestrian-vehicle safety has progressively shifted from crash-based and descriptive analyses toward proactive, conflict-based assessment. Sheykhfard et al. (2021) summarized both passive crash-based and active interaction-based approaches, while Ma et al. (2018) incorporated conflict probability and severity into intersection safety assessment. With the increasing availability of high-resolution trajectory data, recent studies have further advanced toward predicting the evolution of pedestrian-vehicle interactions. Noh et al. (2022) integrated trajectory-related information into predictive collision-risk estimation, while Li et al. (2023) combined vehicle and pedestrian trajectory prediction with probabilistic manoeuver modelling to estimate pedestrian-vehicle conflict risk.

More recent research has increasingly emphasised real-time, interaction-aware, and adaptive risk assessment. Ali et al. (2023) estimated real-time pedestrian crash risk at signalized intersections using Bayesian video analytics, and Wang et al. (2024) developed a real-time vehicle-pedestrian interaction risk model for intersections. Zhao et al. (2025) further incorporated collision-avoidance behaviour into multi-agent trajectory prediction, while Fu et al. (2025) investigated dynamic short-term crash-risk prediction at signalized intersections. Meanwhile, Wu et al. (2025) introduced dynamic thresholds into real-time traffic risk prediction. Most recently, Muduli et al. (2026) have employed a scene-level spatio-temporal graph to predict safety-critical pedestrian-vehicle interactions.

These studies demonstrate a clear transition toward predictive, adaptive, and interaction-aware traffic safety assessment (Tahir & Haque, 2024; Ankunda et al., 2024). Nevertheless, existing advances remain relatively fragmented across different aspects of pedestrian-vehicle safety analysis, and their integrated application for timely and adaptive conflict assessment at signalized intersections remains insufficiently explored. Therefore, this study aims to improve the adaptability and timeliness of pedestrian-vehicle conflict risk assessment at signalized intersections by developing a trajectory-based framework that integrates vehicle trajectory prediction, dynamic safety thresholds, and probabilistic risk estimation. Specifically, this study offers three key contributions: (i) a vehicle trajectory prediction model based on a Hidden Markov Model combined with a greedy algorithm; (ii) the adoption of the minimum extended time-to-collision ($ETTC_{\min}$) as a dynamic conflict indicator with spline-interpolated thresholds; and (iii) a probabilistic framework incorporating driver reaction and braking characteristics.

The remainder of this paper is organised as follows. In Section 2, the material and method are presented, including data acquisition and processing based on field data from a signalized intersection in Xi'an and the SinD dataset, as well as three key technical components: a vehicle trajectory prediction model based on Hidden Markov Models, a dynamic conflict threshold modelling approach using spline interpolation, and a probabilistic collision risk assessment framework integrated with driver reaction and braking times. Section 3 presents the results, evaluating the performance of the framework in terms of prediction accuracy, conflict identification timeliness, and warning consistency. Section 4 provides a comprehensive discussion of the results, analysing the strengths and practical implications of the framework, acknowledging its limitations, and suggesting directions for future research. The conclusions are presented in the final section.

1. Material and method

1.1. Case study and data description

Following established research protocols, the survey site and observation period were selected to ensure the continuity, stability, and reliability necessary for high-precision trajectory data collection. Accordingly, the intersection of Shanglin Road and Caotan 4th Road in Xi'an was selected as the study site. Vehicle and pedestrian trajectory data were obtained from the SinD dataset, which was acquired via UAVs by the School of Vehicle and Mobility at Tsinghua University (Xu et al., 2022).

Spanning morning (7:30–9:30) and evening (16:30–18:30) peak periods, the dataset comprises approximately 3 million valid data points, including 7734 vehicle trajectories and 1528 pedestrian crossing trajectories. With a sampling frequency of 10 Hz and centimetre-level positioning accuracy, the dataset provides a comprehensive record of the motion states and interactive behaviours of both vehicles and pedestrians.

To ensure reliable model training and evaluation while balancing generalization capability, a stratified random sampling method was employed to partition the dataset into training, testing, and validation sets in a 7:2:1 ratio. This approach ensured consistent sample distribution across different time periods and movement states, thereby minimising data bias.

The trajectory dataset consists of naturalistic road-user interactions collected under normal traffic conditions, rather than recorded collision events. Therefore, the proposed framework does not attempt to directly learn crash occurrence. Instead, it identifies potential conflicts by evaluating whether observed or predicted interactions approach critical safety conditions. Accordingly, the historical trajectories are not categorized as “safe” or “collision” trajectories for trajectory-model training. Rather, they are used to characterise normal vehicle motion-transition patterns during naturalistic intersection interactions. Conflict risk is then evaluated from the predicted vehicle–pedestrian interaction states, rather than being assigned as a label to the historical trajectory data.

Figure 1. Intersection of Shanglin Rd. and Caotan Fourth Rd. in Xi’an

1.2. Methodology

To provide an overview of the proposed framework and clarify the relationships among its major components, the complete workflow is illustrated in Figure 2. The framework consists of five sequential stages: sensing and preprocessing, trajectory prediction, conflict assessment, probabilistic risk estimation and grading, and warning output. Vehicle and pedestrian motion states are first obtained from externally sensed trajectory data, after which their future trajectories are predicted over a predefined horizon. The predicted interactions are then evaluated using the minimum extended time-to-collision ($ETTC_{\min}$), which represents the minimum predicted time remaining before vehicle-pedestrian contact over the prediction horizon, together with a dynamic conflict threshold determined according to the real-time vehicle-to-pedestrian ratio, v/p. Identified conflicts are further quantified through a probabilistic model incorporating driver reaction and braking characteristics, and the resulting risk level is used to support roadside, in-vehicle, or traffic-management warnings. As indicated in Figure 2, several components require site- or population-specific calibration when the framework is transferred to different traffic environments, whereas the overall computational structure remains unchanged.

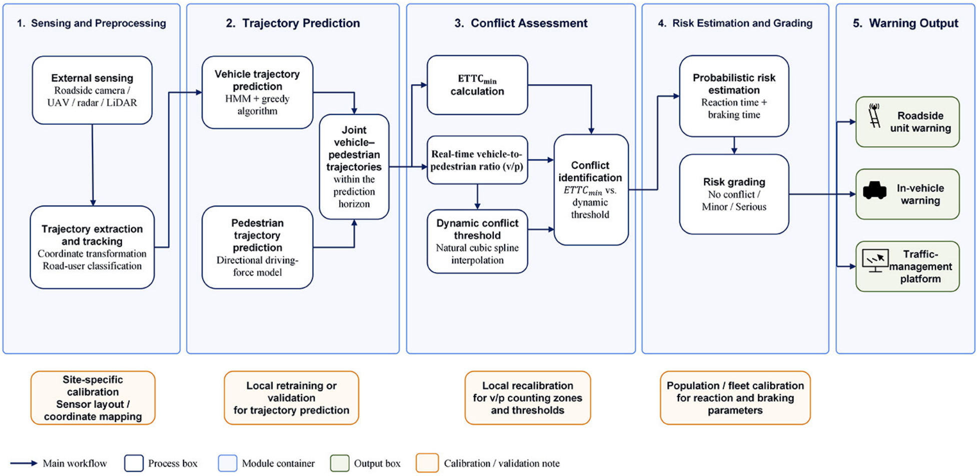

Figure 2. Overall workflow and calibration requirements of the proposed real-time pedestrian-vehicle collision risk warning framework

1.2.1. Vehicle trajectory prediction

This study proposes a trajectory-prediction framework based on a hidden Markov model (HMM), integrating intersection geometry, real-time vehicle states, and historical trajectory data as core inputs. In this framework, geometric characteristics constrain feasible vehicle trajectories, turning behaviours, and speed profiles, and are therefore implicitly reflected in the HMM state-transition probabilities. The framework then extracts motion regularities from historical trajectories to construct the state-transition matrix. It leverages historical motion patterns and employs probabilistic iterative inference combined with a greedy algorithm for trajectory prediction at intersections. Real-time vehicle positions serve as observations, while predicted trajectories are inferred from hidden states through iterative optimisation of transition probabilities (Deng and Söffker, 2021).

The proposed framework is developed from the perspective of a real-time traffic sensing and warning system, in which the motion states of vehicles and pedestrians are obtained from externally observed trajectory information. Based on these kinematic states, the framework predicts their subsequent movements and evaluates the evolution of potential conflicts, thereby allowing risk identification to be performed independently of individual road users' subjective perceptions of the surrounding environment.

To enhance training efficiency and enable real-time prediction, the intersection area is discretized into a spatial grid. The grid resolution was selected to balance accuracy and computational load. While smaller cells (e.g., 5 cm) increase positional precision, they exponentially increase the state space and computational complexity, potentially violating real-time constraints. Conversely, larger cells (e.g., 20 cm) reduce resolution, leading to a degradation in prediction accuracy. Based on experimental validation, a resolution of 10 cm × 10 cm was adopted. Each grid cell corresponds to a hidden state; consequently, the vehicle's measured position at each time step is mapped to the corresponding cell, converting the continuous trajectory into a discrete sequence of observations.

The HMM state-transition matrix is estimated from historical data by quantifying transitions between adjacent cells. The underlying assumption is that short-term vehicle movements at the same intersection exhibit recurrent spatial transition patterns under comparable traffic conditions. Accordingly, historical trajectories are used to estimate feasible motion transitions rather than to prescribe a predetermined safe or risky trajectory. For a given cell x, the probability of moving to a neighbouring cell y is defined as:

$$P\left(x \rightarrow y\right) = \frac{A_{x \rightarrow y}}{\sum_{y \in \mathrm{Neighbors}(x)} A_{x \rightarrow y}}, \tag{1}$$

where $A_{x \rightarrow y}$ represents the frequency of transitions from x to y in the training data, and the denominator represents the total number of transitions from x to all adjacent cells. The set Neighbors(x) denotes the four neighbours (up, down, left, right).

Leveraging the transition and emission structure of the HMM, a greedy iterative algorithm is applied to predict the future trajectory (Liu et al., 2023). Assuming first-order Markov dynamics (where the state at time $n+1$ depends only on the state at time n) and prohibiting immediate reversals to the previous cell, the current state x_{n} is derived from the observation sequence $Z = \{z_1, z_2, z_3, \ldots, z_{\mathrm{n}}\}$. The subsequent position is determined by maximising the transition probability (Figure 3):

$$x_{n+1} = \underset{y \in \mathrm{Neighbors}(x_n)}{\mathrm{argmax}} \; P\left(x_n \rightarrow y\right). \tag{2}$$

This process is iteratively repeated to generate the predicted trajectory $X = \{x_n, x_{n+1}, x_{n+2}, \ldots, x_{n+k}\}$ over the prediction horizon k.

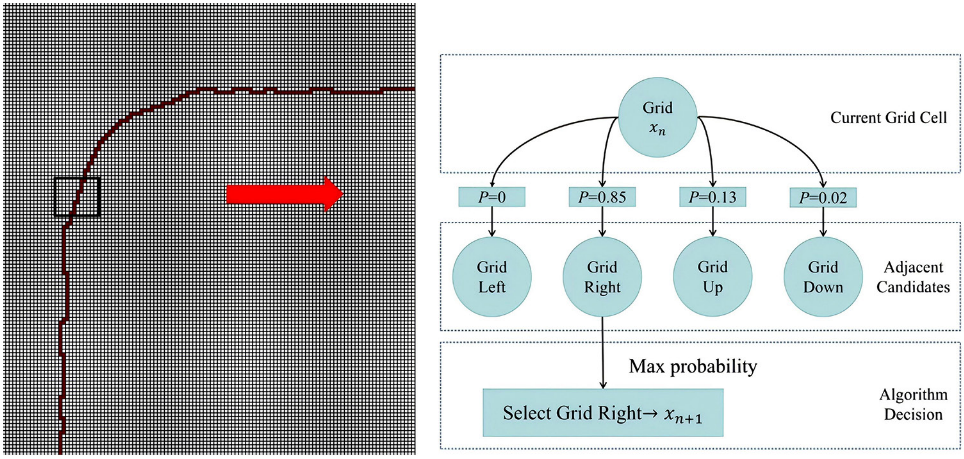

Figure 3. Schematic of greedy algorithm-based grid iteration

1.2.2. Conflict indicator selection

Traffic conflict is defined as a scenario in which two or more road users are on a trajectory to collide in space and time unless at least one alters their course (Abdel-Aty et al., 2023). A conflict is formally detected when a specific conflict indicator exceeds a predefined threshold. By predicting the trajectories of vehicles and pedestrians, the potential collision risk can be quantified.

TTC is a widely adopted metric due to its ease of measurement and analysis. It is primarily applied to rear-end conflicts under the assumption that road users are traveling in the same lane with similar headings and speeds (Gore et al., 2023). However, traditional TTC is ill-suited for conflicts involving lateral interactions or non-following behaviours (Li et al., 2021). To address these limitations, Extended TTC ($ETTC$) generalizes the concept to two-dimensional motion (Ward et al., 2015). By evaluating the coupled planar dynamics of vehicles and pedestrians, $ETTC$ captures complex interactive behaviours, making it superior for unconstrained, two-dimensional interactions and enabling a more comprehensive assessment of conflict risk across diverse traffic scenarios.

To dynamically assess collision risk at time t and capture imminent critical states, we combine the instantaneous states of agents with predicted vehicle trajectories to simulate conflict evolution. The computation of $ETTC_{\min}$ involves propagating the relative motion over multiple future steps – using the predicted vehicle trajectory alongside a pedestrian motion model – and selecting the minimum $ETTC$ value over the prediction horizon as the conflict severity indicator.

Pedestrian crossing behaviour is formulated as a spatial path-optimisation problem. Under free-flow conditions, pedestrians tend to choose the geometrically shortest path to their target. Deviations from this path induce a directional driving force that steers the pedestrian back toward the intended trajectory with a relaxation time constant τ_α. In this study, we adopt a directional driving-force model for pedestrian trajectory prediction (Chen et al., 2019). Unlike the HMM-based vehicle trajectory prediction, pedestrian motion is propagated directly from the currently observed pedestrian position and velocity using the directional driving-force model. The model predicts pedestrian movement toward the intended destination over the prediction horizon. The resulting pedestrian trajectory is then combined with the predicted vehicle trajectory to evaluate their future spatiotemporal interaction and calculate $ETTC_{\min}$. The model is governed by the following equations:

$$\vec{F}_d(t_n) = \frac{1}{\tau_\alpha}\left[v_\alpha^d \frac{\vec{P}_e - \vec{P}_\alpha(t_n)}{\left|\vec{P}_e - \vec{P}_\alpha(t_n)\right|} - \vec{v}_\alpha(t_n) \right], \tag{3}$$

$$\vec{P}_\alpha(t_{n+1}) = \vec{P}_\alpha(t_n) + \vec{v}_\alpha(t_n)\delta t + \vec{F}_d(t_n)(\delta t)^2, \tag{4}$$

where $\vec{P}_\alpha(t_n)$ and $\vec{v}_\alpha(t_n)$ are the pedestrian position and velocity at time t_n, respectively; $\vec{P}_e$ – the target position; $v_\alpha^d = 1.3$ m/s is the desired walking speed; and $\tau_\alpha = 0.5$ s is the relaxation time constant.

Given typical brake-system response times of 200–400 ms (Savitski et al., 2019), we define "persistent braking" as continuous negative acceleration lasting at least 0.5 s (Svärd et al., 2021). The onset of persistent braking marks the conflict start time. At this moment, the position vectors ($\vec{O}$ and $\vec{P}$) and velocity vectors ($\overrightarrow{V_o}$ and $\overrightarrow{V_p}$) of the vehicle and pedestrian are recorded.

Vehicle positions are recorded at the geometric centre. Let d_{op} denote the centre-to-pedestrian Euclidean distance, measured in a top-down coordinate system where all position vectors correspond to projected points on the horizontal plane. To enhance geometric accuracy, we model the vehicle as a rigid rectangle with length L and width W, and the pedestrian as a circle with a typical occupancy radius r (Figure 4a) (Chen et al., 2024). The distance from the pedestrian centre to the closest point on the vehicle's rectangular footprint, d_{op}, is defined as:

$$d_{op} = \max\left\{ D_{op} - \sqrt{\left(\frac{L}{2}\right)^2 + \left(\frac{W}{2}\right)^2} - r, 0 \right\}. \tag{5}$$

For computational convenience, we derive the rate of approach using the centre-based separation rate $\acute{D}_{op}$. Since the dimensions of the vehicle and pedestrian are constant, $\acute{D}_{op} = \acute{d}_{op}$. The pedestrian-vehicle proximity rate is thus:

$$\acute{d}_{op} = \frac{\Delta d_{op}}{\Delta t} = \frac{\Delta D_{op}}{\Delta t} = \frac{\left(\vec{O}-\vec{P}\right)\cdot\left|\vec{V}_o-\vec{V}_p\right|}{\left|\vec{O}-\vec{P}\right|}. \tag{6}$$

The $ETTC$ is calculated to estimate the remaining time until contact between the closest points of the vehicle and pedestrian, assuming constant velocities. As shown in Equation (7), the numerator d_{op} represents the current physical separation accounting for the vehicle's dimensions and the pedestrian's radius. The denominator $\acute{d}_{op}$ represents the rate of change of this separation (i.e., the relative speed projected along the line connecting the two centers). The negative sign ensures that $ETTC$ is positive when the agents are approaching.

$$ETTC = -\frac{d_{op}}{\acute{d}_{op}} = -\frac{D_{op}-\sqrt{\left(\frac{L}{2}\right)^2+\left(\frac{W}{2}\right)^2}-r}{\acute{d}_{op}} = -\frac{\left(\left|\vec{O}-\vec{P}\right|-\sqrt{\left(\frac{L}{2}\right)^2+\left(\frac{W}{2}\right)^2}-r\right)\cdot\left(\vec{O}-\vec{P}\right)}{\left|\vec{O}-\vec{P}\right|\cdot\left|\vec{V}_o-\vec{V}_p\right|}. \tag{7}$$

$ETTC$ is physically meaningful only when the two parties are approaching ($\acute{d}_{op} < 0$) and have not yet overlapped ($d_{op} > 0$). If $d_{op} = 0$, contact has occurred, rendering the metric irrelevant. Conversely, if the agents are stationary or separating ($\acute{d}_{op} \geq 0$), the computed $ETTC$ is negative or infinite and is excluded from the risk assessment.

To analyse the conflict evolution starting at time t, let $\vec{O_1}$ and $\vec{P_1}$ denote the vehicle and pedestrian position vectors at the first prediction step. Trajectories are propagated forward to obtain $\vec{O_i}$ and $\vec{P_i}$ at each step of the prediction horizon. An $ETTC$ value is computed at each step (Figure 4b), and the minimum value, $ETTC_{\min}$, serves as the conflict indicator at time t:

$$ETTC_{\min} = \min\left\{ETTC_1, ETTC_2, \cdots, ETTC_n\right\}. \tag{8}$$

a) *ETTC* calculation schematic **b)** Time-*t* conflict process

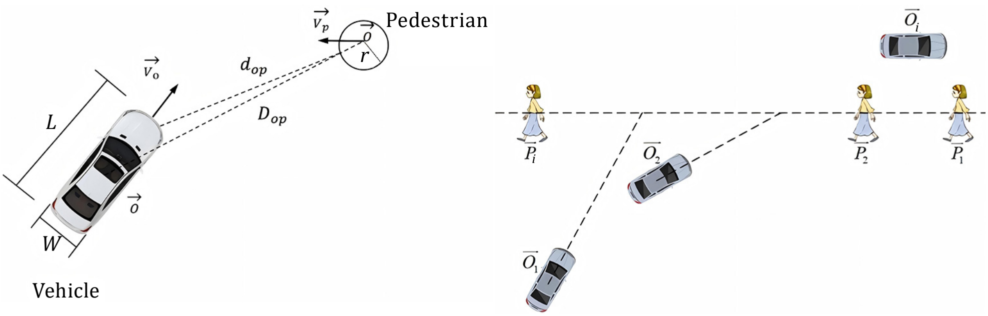

Figure 4. Components of $ETTC_{\min}$ calculation framework

1.2.3. $ETTC_{\min}$ threshold determination

Using pedestrian and vehicle trajectory data, we compute $ETTC_{\min}$ at each time step. While a common traffic engineering practice establishes the conflict threshold at the 85th percentile of the cumulative distribution (Karimi et al., 2021), intersection-specific characteristics often necessitate adjustments. To accurately capture how conflict risk varies with road-user density and interaction patterns, we partition each entry approach into three canonical conflict scenarios. In this study, the south approach refers to the entry leg on the southern side of the intersection, where vehicles approach the intersection from south to north. Using this approach as an example, three canonical conflict scenarios are considered:

- Scenario 1 (Left-Turn Conflict): Interactions between left-turning vehicles from the south approach and pedestrians crossing the south or west approaches;
- Scenario 2 (Through Conflict): Interactions between through-moving vehicles from the south approach and pedestrians crossing the south or north approaches;
- Scenario 3 (Right-Turn Conflict): Interactions between right-turning vehicles from the south approach and pedestrians crossing the south or east approaches.

For each scenario, we analyse the influence of the vehicle-to-pedestrian ratio (v/p) on the $ETTC_{\min}$ threshold. The ratio v/p is defined as the number of vehicles involved in a specific conflict sequence divided by the number of pedestrians on the relevant crosswalk. Specifically, this metric accounts for all vehicles executing a specific movement while pedestrians are present in or approaching the conflict zone. Unlike fixed observation windows, this ratio captures the instantaneous interaction intensity, serving as a real-time indicator of the competitive pressure and behavioural adaptations that define the accepted safety margin.

The adoption of v/p as a dynamic scaling factor is grounded in traffic flow theory and behavioural research. High v/p values signify increased vehicle dominance, often correlating with competitive driver behaviour, reduced yielding compliance, and shorter accepted safety margins (Papazikou et al., 2017). Consequently, the effective conflict threshold decreases. Conversely, a low v/p value indicates pedestrian predominance, which can increase pedestrian assertiveness and crossing unpredictability. This shift in the risk profile necessitates threshold recalibration to minimize false alarms. Static thresholds, such as the conventional 85th percentile, fail to account for these dynamic behavioural adjustments, potentially leading to missed detections or reduced specificity. By modulating the $ETTC_{\min}$ threshold based on v/p, the proposed system maintains sensitivity and precision across diverse interaction scenarios.

To model the functional relationship between the threshold and *v/p*, we employ natural cubic spline interpolation. Given N observations (x_i, y_i), $i = 1, 2, \ldots, N$, where x_i represents the ratio *v/p* and y_i the corresponding threshold, the domain $[x_{\min}, x_{\max}]$ is partitioned into M subintervals. Knots are defined at the midpoints of adjacent data points:

$$\xi_k = \frac{1}{2}\left(x_k + x_{k+1}\right)\left(k = 0,1,\ldots,M\right), \text{ with } \xi_0 = x_{\min} \text{ and } \xi_M = x_{\max}. \tag{9}$$

On each subinterval $\left[\xi_k, \xi_{k+1}\right]$, we define a cubic function:

$$S_k\left(x\right) = a_k + b_k\left(x - \xi_k\right) + c_k(x - \xi_k)^2 + d_k(x - \xi_k)^3. \tag{10}$$

Natural boundary conditions are applied to ensure a unique solution:

$$S''0\left(\xi_0\right) = S''M - 1\left(\xi_M\right) = 0. \tag{11}$$

The resulting spline $S(x)$ is C^2-continuous, ensuring smoothness while providing high fitting accuracy and locality, where local data variations affect only neighbouring intervals (Shi & Li, 2023). This function establishes the $ETTC_{\min}$ threshold as a function of *v/p* for each scenario, enabling the dynamic classification of pedestrian-vehicle conflicts.

1.2.4. Probability estimation of collision risk

A lower $ETTC_{\min}$ value indicates a higher conflict risk and a greater likelihood of a pedestrian-vehicle collision (Mahmud et al., 2017). To assess collision potential at intersections, we compare $ETTC_{\min}$ with the required stopping time, defined as the sum of the driver's reaction time (T_f) and braking time (T_z). In the proposed framework, conflict recognition and driver response are modeled as distinct processes: potential conflicts are identified from externally observed vehicle-pedestrian trajectories, whereas the reaction-time term represents the behavioural delay in the driver's response after conflict-related information becomes available. Assuming a constant deceleration rate $a_i > 0$ from an initial speed v_i, the braking time is calculated as $T_z = v_i / a_i$.

The driver reaction time, T_f, is modelled as a Gaussian random variable with a mean of 2.29 s and a standard deviation of 0.32 s (Li et al., 2019), representing the overall response delay from conflict perception to braking initiation. These parameters provide a baseline representation of human-driver response rather than a fleet-specific calibration. Accordingly, the probabilistic formulation treats reaction and braking characteristics as configurable components, allowing their parameters to be recalibrated when the framework is applied to traffic environments with different driver populations or vehicle-response characteristics. Its probability density function (PDF) is given by:

$$f\left(T_f\right)=\frac{1}{0.32\sqrt{2\pi}}\exp\left[-\frac{(T_f-2.29)^2}{2\times\left(0.32\right)^2}\right]. \tag{12}$$

A collision is predicted when $ETTC_{\min} < T_f + T_z$, implying that the remaining time is insufficient for the driver to react and brake effectively. The probability of collision is therefore derived as the complement of the probability that the driver stops safely (i.e., when available time exceeds required time):

$$P\left(ETTC_{\min}<T_f+T_z\right)=1-P\left(ETTC_{\min}\geq T_f+T_z\right), \tag{13}$$

$$P\left(ETTC_{\min}<T_f+T_z\right)=1-\int_{\max\left(0,ETTC_{\min}-T_z\right)}^{+\infty} f\left(T_f\right)\mathrm{d}T_f, \tag{14}$$

$$P\left(ETTC_{\min}<T_f+T_z\right)=1-\Phi\left[\frac{\left(ETTC_{\min}-T_z\right)-2.29}{0.32}\right], \tag{15}$$

where Φ is the standard normal cumulative distribution function.

2. Results

2.1. Test of vehicle trajectory prediction

To evaluate the performance of the HMM-based vehicle trajectory prediction method across different driving behaviours, we quantified performance using average displacement error (ADE), path similarity (PS), trajectory coverage (TC), and trajectory direction error (TDE) (Shi et al., 2019). These metrics were computed on the test set, with results summarised in Table 1. Overall, the model demonstrates robust performance across all behaviours. Although prediction accuracy for right-turn vehicles is slightly lower than for through and left-turn movements – likely due to the absence of signal control and greater exposure to external disturbances – the consistently favourable results across all metrics confirm the model's effectiveness and robustness under varied conditions.

Table 1. Evaluation of vehicle trajectory prediction accuracy

Vehicle operating condition	ADE, m	PS	TC, %	TDE, °
Left-turning trajectory	0.5746	0.9425	95.24	0.4357
Straight trajectory	0.3254	0.9786	98.25	0.2486
Right-turning trajectory	0.6879	0.9357	93.98	0.5791

To evaluate the trajectory prediction method in real-time collision warning scenarios and verify its balance of accuracy and efficiency, we compared the proposed HMM against four widely used machine learning models using the test set: Long Short-Term Memory (LSTM), Transformer, Graph Neural Network (GNN), and Multi-Layer Perceptron (MLP). Average Displacement Error (ADE) served as the primary metric for accuracy, presented as intervals to reflect performance variations across different turning manoeuvers. Additionally, inference time per query and parameter count were recorded to assess computational efficiency and deployment feasibility.

As shown in Table 2, while the LSTM and Transformer models achieve slightly lower ADE in certain scenarios – indicating marginally superior accuracy – the proposed HMM offers a more competitive balance between predictive performance and computational efficiency. Notably, the HMM exhibits significantly lower inference latency than the LSTM and Transformer, rendering it more suitable for real-time collision warning systems where rapid response is critical. The GNN demonstrates moderate performance but incurs higher computational overhead than the HMM. Finally, although the MLP offers the fastest inference speeds, it yields substantially higher ADE – particularly during complex turning manoeuvers – due to its limited ability to capture sequential dependencies. This limitation restricts its utility for high-fidelity trajectory prediction.

Table 2. Performance comparison of trajectory prediction models

Model	ADE, m	Inference time, ms/query	Number of parameters, $\times 10^4$
HMM	0.31–0.71	8–12	0.8
LSTM	0.28–0.65	35–42	12.5
Transformer	0.25–0.61	89–105	48.3
GNN	0.30–0.67	41–48	15.7
MLP	0.72–1.05	5–7	0.5

2.2. Refining the evaluation of conflict indicators

To rigorously assess the improvement in conflict metrics for pedestrian-vehicle interactions, this study compares the proposed $ETTC_{\min}$ with the conventional TTC. A representative conflict event was extracted from the test set, and the temporal evolution of both metrics was computed and plotted as a function of time (Figure 5).

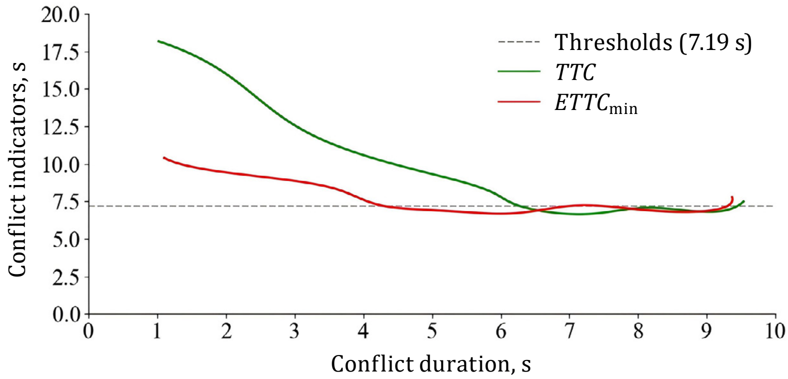

Figure 5. Plot of $ETTC_{\min}$ versus TTC

Based on a ratio v/p of 5:1, spline interpolation determined a conflict threshold of 7.19 s; values of TTC or $ETTC_{\min}$ at or below this level signify a hazardous condition. Under this criterion, the TTC identifies the hazard at 6.11 s, whereas $ETTC_{\min}$ detects it significantly earlier at 4.35 s, providing a 1.76 s advance warning. Consequently, compared to the traditional crash-time metric, $ETTC_{\min}$ facilitates earlier hazard detection, granting road users critical additional time for evasive actions such as deceleration or lane adjustments. This extended reaction window contributes to enhanced driving safety and a potential reduction in crash frequency.

2.3. Conflict classification results

The processed $ETTC_{\min\ \text{values}}$ from the test set were input into the collision probability model to estimate the likelihood of vehicle-pedestrian collisions (Table 3).

Table 3. Vehicle-pedestrian collision probability distribution

Collision probability interval	Frequency	Proportion, %
0.0–0.1	15303	84.33
0.1–0.2	820	4.52
0.2–0.3	320	1.76
0.3–0.4	237	1.31
0.4–0.5	199	1.09
0.5–0.6	195	1.07
0.6–0.7	204	1.12
0.7–0.8	221	1.22
0.8–0.9	263	1.45
0.9–1.0	386	2.13

The resulting probability distribution indicates that the majority of pedestrian-vehicle interactions maintain a collision probability below 10%, reflecting a generally low-risk environment. In such scenarios, sufficient time remains for evasive manoeuvers, minimizing the likelihood of severe outcomes. Consequently, interactions with a collision probability below 10% are classified as minor conflicts, while those exceeding 10% represent a substantially higher risk and are classified as serious conflicts.

To evaluate the consistency between predicted risks and observed conflicts, kinematically defined conflicts were identified using evasive-behaviour indicators. Prior studies suggest that abrupt braking or steering behaviours signify risk-avoidance manoeuvers indicative of actual conflicts (Nie et al., 2021). Accordingly, an interaction is defined as a conflict if either party exhibits significant evasive behaviour: specifically, if the vehicle's absolute acceleration exceeds 4 m/s^2 or its heading change exceeds 30°, or if the pedestrian's acceleration exceeds 1 m/s^2 or their heading change exceeds 45° (Lenard et al., 2018). Events where only one party meets these criteria are labelled minor conflicts, whereas events where both parties exhibit such behaviour are labelled serious conflicts. Figure 6 presents a heat map comparing the conflicts predicted by the proposed method with the observed kinematically defined conflicts in the validation set.

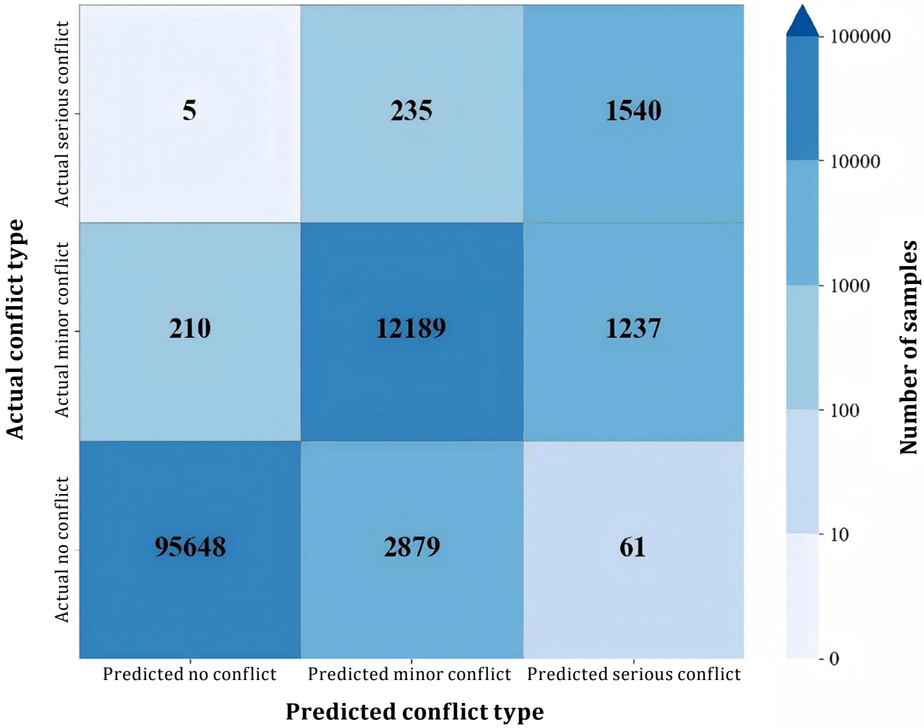

Figure 6. Comparison between predicted conflicts and kinematically defined observed conflicts

The proposed collision-warning method demonstrates strong agreement with observed outcomes, achieving an overall consistency rate of 95.94%. Among the discrepancies, 2.53% were false positives (predicted as minor conflicts but observed as no conflict), and 1.14% were overestimations (predicted as serious but observed as minor or no conflict). These deviations may stem from environmental factors, driver heterogeneity, or other stochastic elements that influence the comparability of predictions and observations (Ma et al., 2024). Crucially, underestimation – instances where the observed conflict was more severe than predicted – occurred in fewer than 0.4% of cases, indicating that the system rarely fails to identify high-risk events. Consequently, the method demonstrates promising capability for real-time conflict warning at intersections based on surrogate safety assessment.

The empirical analysis based on the dataset further validates the effectiveness of the proposed approach. The HMM-based trajectory prediction model maintained high accuracy across left-turn, through, and right-turn movements, demonstrating adaptability to diverse driving behaviours. In terms of timeliness, the $ETTC_{\min}$

metric identified potential hazards earlier than conventional *TTC* in examined cases, with one representative conflict showing an advance warning of 1.76 s. Furthermore, the use of a spline-interpolated dynamic threshold addressed the limitations of the traditional 85th-percentile cumulative-frequency threshold under varying v/p conditions, enhancing the robustness of conflict identification. These findings are corroborated by the collision-probability distribution and heat map analysis, where the 95.94% alignment between predicted and observed kinematically defined conflicts demonstrates the effectiveness of the proposed warning framework.

3. Discussion

3.1. Performance and mechanistic analysis

The proposed trajectory prediction framework, which integrates an HMM with a greedy algorithm, demonstrates robust performance across typical intersection manoeuvers, despite discernible variations in predictive accuracy. These performance differences are largely attributable to the inherent compatibility between specific motion constraints and the model's foundational assumptions. For through and left-turn movements, vehicle trajectories are predominantly governed by traffic signal controls, resulting in highly regular and predictable motion patterns. Such regularity aligns well with the first-order Markovian state transition assumption of the HMM (He et al., 2023), thereby facilitating accurate predictions. In contrast, right-turn manoeuvers often occur without strict signal control, rendering them more susceptible to external disturbances, such as interactions with crossing pedestrians or non-motorized vehicles. This susceptibility introduces greater stochasticity into state transitions, consequently diminishing prediction accuracy. However, the model's ability to capture short-term motion dependencies is highly congruent with the dynamic nature of vehicle movements at intersections, which are often characterized by rapid, short-cycle directional changes (Zhang et al., 2023). This scenario-specific adaptability underscores the model's utility, particularly at intersections where right-turn interference is minimal.

Regarding conflict identification, the $ETTC_{\min}$ indicator offers a significant improvement in timeliness compared to the conventional *TTC*. This enhancement stems from the indicator's basis in two-dimensional dynamics. Restricted to longitudinal kinematics, traditional *TTC* fails to adequately assess risks in lateral or oblique encounters, such as those involving turning vehicles and diagonally crossing pedestrians (Park et al., 2025). In contrast, $ETTC_{\min}$ integrates both longitudinal and lateral velocity components, enabling a holistic evaluation of the planar coupled motion between road users. Furthermore, unlike *TTC*, which relies on a single instantaneous state calculation, $ETTC_{\min}$ proactively identifies the most critical point of potential collision within a prediction horizon. By focusing on the $ETTC_{\min}$, the method ensures that localized high-risk situations are not obscured by averaged states. This enhances warning sensitivity and aligns with the principle that conflict metrics should prioritize critical risk moments (Peng & Liu, 2026). The advance warning time provided by $ETTC_{\min}$ is particularly valuable as it correlates closely with typical driver reaction times (Li et al., 2019), offering a practical window for evasive action and addressing the limitations of TTC in complex, non-following interaction scenarios.

In terms of threshold determination and risk assessment, the dynamic threshold mechanism – established via natural cubic spline interpolation – exhibits superior environmental adaptability compared to static percentile-based thresholds (Arun et al., 2021). By continuously adjusting the conflict threshold in response to the real-time ratio *v/p*, the method effectively captures the evolving nature of intersection risk under varying traffic densities. The continuity and local adaptability inherent in the spline function (Shi & Li, 2023) prevent overfitting to noisy data while ensuring the threshold responds appropriately to gradient changes in interaction frequency. This dynamic approach, combined with a probabilistic collision risk model that incorporates driver reaction time and braking characteristics, addresses a recognized gap in static threshold applications, which often struggle with false or missed warnings in dynamic environments (Wu et al., 2025). The probabilistic output facilitates a refined, interpretable risk grading, enabling targeted safety interventions (Wali et al., 2020; Reinmueller et al., 2020). The high consistency between predicted and observed conflicts, coupled with a minimal rate of underestimation for high-risk events, validates the robustness and practical reliability of this integrated assessment framework.

Although the framework is trajectory-based, it partially incorporates human behavioural responses through naturalistic vehicle trajectories, pedestrian directional adaptation, probabilistic driver-response modelling, and validation based on evasive behaviour. Overall, the proposed framework demonstrates strong robustness across different conflict-severity levels. Its high consistency in identifying non-conflict and serious-conflict events can be attributed to their distinct interaction characteristics, whereas minor conflicts involve greater uncertainty because of overlapping behavioural patterns and stochastic traffic interactions. These inherent complexities underscore the challenge of achieving perfect prediction accuracy in real-world pedestrian-vehicle interactions (Lin et al., 2024; Wang et al., 2025).

3.2. Strengths and implications

The core strength of this method lies in its proactive nature. Rather than relying on historical crash data, the framework utilises real-time trajectory prediction and dynamic conflict indicators for risk assessment. This allows traffic management authorities to identify potential high-risk configurations and conflict points during the intersection planning phase or when evaluating newly built intersections. Consequently, interventions can be implemented at the design source to optimise traffic organisation and physical layout, shifting the paradigm from reactive response to proactive prevention and significantly enhancing the scientific rigor of safety management.

Owing to the relatively low computational complexity of the HMM and the greedy algorithm, the framework exhibits excellent real-time performance. This capability enables seamless integration into existing intelligent transportation infrastructure, such as roadside units, or deployment as part of in-vehicle warning systems (Ding et al., 2024). Because conflict identification is based on externally sensed road-user trajectories, the warning process does not depend solely on the driver's direct visual recognition of the interacting pedestrian. This feature is particularly valuable in complex intersection scenarios, where timely risk information can be provided before the driver initiates an evasive response.

Moreover, trajectory-based conflict identification and subsequent vehicle-response estimation are treated as separate components, providing additional flexibility for practical deployment. When the framework is applied to regions with different fleet characteristics, the reaction-time and braking parameters can be recalibrated according to local driving behaviour and vehicle-response characteristics without modifying the trajectory-prediction, $ETTC_{\min}$, or dynamic-threshold components. For vehicles equipped with active safety functions, assisted or automated responses can similarly be incorporated through appropriate response-related parameterization. This modular structure enables the framework to accommodate heterogeneous vehicle technologies while preserving its core trajectory-based risk-identification mechanism, thereby supporting its application across diverse traffic environments.

Finally, the output of this method is not a simple binary alert but an interpretable, graded warning based on collision probability. For instance, using a 10% probability threshold to distinguish between minor and serious conflicts provides clear and actionable insights. Based on this information, management departments can implement targeted interventions, such as focusing control efforts on high-risk conflict types, optimising signal timing for specific approaches, or installing visual warning devices at critical locations. This approach optimises the allocation of management resources and improves the precision and efficiency of safety interventions.

Although the framework was developed using data from a specific signalized intersection, its deployment is not limited to this configuration. The methodological structure is transferable; however, scenario-dependent parameters, such as the HMM transition matrix and dynamic $ETTC_{\min}$ thresholds, require local recalibration according to intersection geometry, traffic conditions, and road-user behaviour. Thus, practical implementation can be achieved through site-specific calibration rather than by directly transferring parameters derived from a single intersection. To further clarify the transferability of individual framework components and the corresponding requirements for practical deployment, Table 4 summarises which components can retain their methodological structure and which require site-, population-, or fleet-specific recalibration when applied to a new traffic environment.

Table 4. Transferability and adaptation strategy of the proposed framework across intersection environments

Framework component	Transferability level	Elements retained across sites	Site-specific update, if needed	Main adaptation basis
Overall framework architecture	High	Five-stage workflow from sensing and trajectory prediction to conflict assessment, probabilistic risk estimation, and warning output	None at the methodological level	Deployment configuration
Vehicle trajectory prediction	High at the methodological level	HMM-based prediction structure, spatial-state representation, and greedy prediction procedure	Re-estimation of the HMM transition matrix where local motion patterns differ	Local vehicle trajectories, intersection geometry, and traffic control
Pedestrian trajectory prediction	Generally transferable	Directional driving-force formulation and prediction procedure	Parameter validation or adjustment only when pedestrian behaviour differs substantially	Local walking speed, crossing patterns, and destination characteristics
$ETTC_{\min}$ calculation	Directly transferable	Computational formulation and conflict-severity definition	No model recalibration; local trajectory and geometric inputs are updated during operation	Real-time vehicle–pedestrian kinematic states
Dynamic conflict threshold based on *v/p*	Method transferable; calibration site-dependent	*v/p*-based adaptive threshold mechanism and natural cubic spline formulation	Re-estimation of the local *v/p*–$ETTC_{\min}$ threshold relationship	Local interaction intensity and conflict distributions
Conflict identification	Directly transferable	Decision logic comparing $ETTC_{\min}$ with the dynamic threshold	Automatically follows the locally calibrated threshold	Predicted interaction states and dynamic threshold
Probabilistic collision-risk estimation	High at the model level	Probabilistic formulation linking available conflict time with reaction and braking time	Response parameters may be recalibrated when driver population or fleet characteristics differ	Driver reaction characteristics, braking performance, and fleet composition
Risk grading and warning output	Generally transferable	Probability-based grading concept and multi-channel warning architecture	Operational cutoffs may be validated according to local management objectives	Warning tolerance and traffic-management requirements

3.3. Limitations and future research

Despite these encouraging results, several issues warrant further investigation. First, the framework was developed and validated using data from a single two-phase signalized intersection. Further evaluation across diverse intersection layouts, control strategies, and multimodal traffic environments is therefore needed to assess its broader generalizability. Second, human behavioural adaptation is represented in a simplified manner. Although naturalistic motion patterns, pedestrian directional adaptation, and stochastic driver responses are incorporated, the continuous perception–decision–action process, driver-specific visibility constraints, and technology-related response differences are not explicitly modelled. Future research could incorporate more interaction-aware behavioural models and locally calibrated response parameters. Finally, the current validation is based on kinematically defined surrogate conflicts rather than observed crash outcomes. Future studies should evaluate the framework using broader multi-site safety datasets and, where detailed data are available, further examine the effects of intersection geometry and vehicle operating characteristics.

Conclusion

The real-time pedestrian-vehicle collision risk warning framework proposed in this study was developed to enhance the adaptability and timeliness of pedestrian-vehicle conflict risk assessment at signalized intersections. The framework integrates HMM-based trajectory prediction, dynamic threshold modelling, and collision probability estimation. Its methodological contribution lies in combining short-term trajectory prediction with $ETTC_{\mathrm{min}}$-based conflict assessment, dynamically adjusting conflict thresholds according to the real-time vehicle-to-pedestrian ratio, and incorporating driver reaction and braking characteristics into probabilistic risk estimation. The dynamic threshold mechanism improves adaptability to varying interaction conditions, while trajectory prediction enables earlier identification of potential conflicts. In addition, probabilistic risk estimation extends conflict assessment beyond purely kinematic threshold-based identification by accounting for driver reaction and braking behaviour. Empirical validation demonstrates that the proposed method achieves high trajectory prediction accuracy, rapid conflict identification, and consistent warning performance, thereby providing real-time technical support for intersection safety management.

Funding

This work was supported by the Fundamental Research Funds for the Central Universities of Chang'an University (number 300102345601).

Author Contributions

Haoliang Shen: Investigation; Methodology; Formal analysis; Validation; Writing – original draft. Yuquan Meng: Data curation; Formal analysis; Validation. Yihe Huo: Methodology; Writing – review and editing. Yonggang Wang: Conceptualization; Supervision; Funding acquisition; Writing – review and editing.

Disclosure Statement

The authors declare that they have no known competing financial interests or personal relationships that could have appeared to influence the work reported in this paper.

Statement of the use of generative AI and AI-assisted technologies in the writing process

During the preparation of this manuscript, the authors used AI-assisted tools only for language polishing, grammar improvement, and minor formatting support, while the research design, data analysis, modelling, interpretation of results, conclusions, and final manuscript content were developed, verified, and approved by the authors; no AI tool was used to generate original research data, fabricate results, or alter the scientific findings, and the authors take full responsibility for the content of the manuscript.

REFERENCES

Abdel-Aty, M., Wang, Z., Zheng, O., & Abdelraouf, A. (2023). Advances and applications of computer vision techniques in vehicle trajectory generation and surrogate traffic safety indicators. *Accident Analysis and Prevention*, *191*, Article 107191. https://doi.org/10.1016/j.aap.2023.107191

Ali, Y., Haque, M. M., & Mannering, F. (2023). A Bayesian generalised extreme value model to estimate real-time pedestrian crash risks at signalised intersections using artificial intelligence-based video analytics. *Analytical Methods in Accident Research*, *38*, Article 100264. https://doi.org/10.1016/j.amar.2022.100264

Ankunda, A., Ali, Y., & Mohanty, M. (2024). Pedestrian crash risk analysis using extreme value models: New insights and evidence. *Accident Analysis and Prevention*, *203*, Article 107633. https://doi.org/10.1016/j.aap.2024.107633

Arun, A., Haque, M. M., Bhaskar, A., Washington, S., & Sayed, T. (2021). A systematic mapping review of surrogate safety assessment using traffic conflict techniques. *Accident Analysis and Prevention*, *153*, Article 106016. https://doi.org/10.1016/j.aap.2021.106016

Chen, P., Zeng, W., & Yu, G. (2019). Assessing right-turning vehicle-pedestrian conflicts at intersections using an integrated microscopic simulation model. *Accident Analysis and Prevention*, *129*, 211–224. https://doi.org/10.1016/j.aap.2019.05.018

Chen, X., Li, S., Yang, W., Chen, Y., & Wang, H. (2024). Enhanced microsimulation framework for right-turning vehicle-pedestrian interactions at signalized intersection. *Simulation Modelling Practice and Theory*, *134*, Article 102930. https://doi.org/10.1016/j.simpat.2024.102930

Deng, Q., & Söffker, D. (2021). A review of HMM-based approaches of driving behaviors recognition and prediction. *IEEE Transactions on Intelligent Vehicles*, *7*(1), 21–31. https://doi.org/10.1109/TIV.2021.3065933

Ding, H., Sun, Y., Wang, L., Zheng, X., Huang, W., & Lu, X. (2024). Intersection eco-driving strategies under mixed traffic environment: A novel cooperation of traffic signal and vehicle trajectory planning. *Physica A: Statistical Mechanics and its Applications*, *655*, Article 130203. https://doi.org/10.1016/j.physa.2024.130203

Fu, C., Lu, Z., Liu, H., & Wumaierjiang, A. (2025). Dynamic short-term crash risk prediction from traffic conflicts at signalized intersections with emerging mixed traffic flow: A novel conflict indicator. *Accident Analysis and Prevention*, *217*, Article 108065. https://doi.org/10.1016/j.aap.2025.108065

Gore, N., Chauhan, R., Easa, S., & Arkatkar, S. (2023). Traffic conflict assessment using macroscopic traffic flow variables: A novel framework for real-time applications. *Accident Analysis and Prevention*, *185*, Article 107020. https://doi.org/10.1016/j.aap.2023.107020

He, Z., Ning, L., Jiang, B., Li, J., & Wang, X. (2023). Vehicle intersections prediction based on Markov model with variable weight optimization. *Sustainability*, *15*(8), Article 6943. https://doi.org/10.3390/su15086943

Karimi, A., Boroujerdian, A. M., & Amini, I. (2021). Risk evaluation of multiple passing maneuvers on two-lane rural highways in Iran. *Accident Analysis and Prevention*, *163*, Article 106472. https://doi.org/10.1016/j.aap.2021.106472

Lenard, J., Welsh, R., & Danton, R. (2018). Time-to-collision analysis of pedestrian and pedal-cycle accidents for the development of autonomous emergency braking systems. *Accident Analysis and Prevention*, *115*, 128–136. https://doi.org/10.1016/j.aap.2018.02.028

Li, P., Guo, H., Bao, S., & Kusari, A. (2023). A probabilistic framework for estimating the risk of pedestrian-vehicle conflicts at intersections. *IEEE Transactions on Intelligent Transportation Systems*, *24*(12), 14111–14120. https://doi.org/10.1109/TITS.2023.3296567

Li, X., Rakotonirainy, A., & Yan, X. (2019). How do drivers avoid collisions? A driving simulator-based study. *Journal of Safety Research*, *70*, 89–96. https://doi.org/10.1016/j.jsr.2019.05.002

Li, Y., Wu, D., Chen, Q., Lee, J., & Long, K. (2021). Exploring transition durations of rear-end collisions based on vehicle trajectory data: A survival modeling approach. *Accident Analysis and Prevention*, *159*, Article 106271. https://doi.org/10.1016/j.aap.2021.106271

Lin, C., Zhang, S., Gong, B., & Liu, H. (2024). Near-crash risk identification and evaluation for takeout delivery motorcycles using roadside LiDAR. *Accident Analysis and Prevention*, *199*, Article 107520. https://doi.org/10.1016/j.aap.2024.107520

Liu, P., Qu, T., Gao, H., & Gong, X. (2023). Driving intention recognition of surrounding vehicles based on a time-sequenced weights hidden Markov model for autonomous driving. *Sensors*, *23*(21), Article 8761. https://doi.org/10.3390/s23218761

Ma, Q., Zhang, S., & Zhou, Q. (2021). Development of a conflict-free unsignalized intersection organization method for multiple connected and autonomous vehicles. *Plos One*, *16*(3), Article e0249170. https://doi.org/10.1371/journal.pone.0249170

Ma, S., Xu, S., Song, J., Wang, K., Qin, H., & Wang, R. (2024). Study on driver's active emergency response in dangerous traffic scenes based on driving simulator. *Traffic Injury Prevention*, *25*(2), 116–121. https://doi.org/10.1080/15389588.2023.2282948

Ma, Y., Qin, X., Grembek, O., & Chen, Z. (2018). Developing a safety heatmap of uncontrolled intersections using both conflict probability and severity. *Accident Analysis and Prevention*, *113*, 303–316. https://doi.org/10.1016/j.aap.2018.01.038

Mahmud, S. S., Ferreira, L., Hoque, M. S., & Tavassoli, A. (2017). Application of proximal surrogate indicators for safety evaluation: A review of recent developments and research needs. *IATSS Research*, *41*(4), 153–163. https://doi.org/10.1016/j.iatssr.2017.02.001

Muduli, K., Ghosh, I., & Ukkusuri, S. V. (2026). A graph-based spatio-temporal framework for predicting safety-critical pedestrian-vehicle interactions at unsignalized crosswalks. *Accident Analysis and Prevention*, *228*, Article 108409. https://doi.org/10.1016/j.aap.2026.108409

Nie, B., Li, Q., Gan, S., Xing, B., Huang, Y., & Li, S. E. (2021). Safety envelope of pedestrians upon motor vehicle conflicts identified via active avoidance behaviour. *Scientific Reports*, *11*(1), Article 3996. https://doi.org/10.1038/s41598-021-82331-z

Noh, B., Park, H., & Yeo, H. (2022). Analyzing vehicle-pedestrian interactions: Combining data cube structure and predictive collision risk estimation model. *Accident Analysis and Prevention*, *165*, Article 106539. https://doi.org/10.1016/j.aap.2021.106539

Papazikou, E., Quddus, M., & Thomas, P. (2017). Detecting deviation from normal driving using SHRP2 NDS data. *Annual Meeting of Transportation Research Board*. Washington D.C., US. https://repository.lboro.ac.uk/articles/conference_contribution/Detecting_deviation_from_normal_driving_using_SHRP2_NDS_data/9340919?file=16949609

Park, N., Park, J., Joo, Y. J., & Abdel-Aty, M. (2025). Micro-level hotspot identification at intersections using traffic conflict analysis. *Accident Analysis and Prevention*, *220*, Article 108167. https://doi.org/10.1016/j.aap.2025.108167

Peng, T., & Liu, J. (2026). Analysis of conflict between right-turning vehicles and pedestrians at urban intersections using random parameter Logit model. *Traffic Injury Prevention*, *27*(6), 735–743. https://doi.org/10.1080/15389588.2025.2545001

Reinmueller, K., Kiesel, A., & Steinhauser, M. (2020). Adverse behavioral adaptation to adaptive forward collision warning systems: An investigation of primary and secondary task performance. *Accident Analysis and Prevention*, *146*, Article 105718. https://doi.org/10.1016/j.aap.2020.105718

Savitski, D., Ivanov, V., Augsburg, K., Shyrokau, B., & Fujimoto, H. (2019). Recent advancements in continuous wheel slip control. *The IAVSD International Symposium on Dynamics of Vehicles on Roads and Tracks*, 1525–1535. https://doi.org/10.1007/978-3-030-38077-9_175

Sheykhfard, A., Haghighi, F., Papadimitriou, E., & Van Gelder, P. (2021). Review and assessment of different perspectives of vehicle-pedestrian conflicts and crashes: Passive and active analysis approaches. *Journal of Traffic and Transportation Engineering* (English Edition), *8*(5), 681–702. https://doi.org/10.1016/j.jtte.2021.08.001

Shi, X., Wong, Y. D., Li, M. Z. F., Palanisamy, C., & Chai, C. (2019). A feature learning approach based on XGBoost for driving assessment and risk prediction. *Accident Analysis and Prevention*, *129*, 170–179. https://doi.org/10.1016/j.aap.2019.05.005

Shi, X., & Li, X. (2023). Trajectory planning for an autonomous vehicle with conflicting moving objects along a fixed path – An exact solution method. *Transportation Research Part B: Methodological*, *173*, 228–246. https://doi.org/10.1016/j.trb.2023.05.001

Svärd, M., Markkula, G., Bärgman, J., & Victor, T. (2021). Computational modeling of driver pre-crash brake response, with and without off-road glances: Parameterization using real-world crashes and near-crashes. *Accident Analysis and Prevention*, *163*, Article 106433. https://doi.org/10.1016/j.aap.2021.106433

Tahir, H. B., & Haque, M. M. (2024). A non-stationary bivariate extreme value model to estimate real-time pedestrian crash risk by severity at signalized intersections using artificial intelligence-based video analytics. *Analytic Methods in Accident Research*, *43*, Article 100339. https://doi.org/10.1016/j.amar.2024.100339

Wali, B., Khattak, A. J., & Karnowski, T. (2020). The relationship between driving volatility in time to collision and crash-injury severity in a naturalistic driving environment. *Analytic Methods in Accident Research*, *28*, Article 100136. https://doi.org/10.1016/j.amar.2020.100136

Wang, T., Ge, Y. E., Wang, Y., Chen, W., Fu, Q., & Niu, Y. (2024). A novel model for real-time risk evaluation of vehicle-pedestrian interactions at intersections. *Accident Analysis and Prevention*, *206*, Article 107727. https://doi.org/10.1016/j.aap.2024.107727

Wang, T., Ma, L., & Ma, X. (2025). Emergency scenario evolution of Arctic maritime accidents using data-driven dynamic Bayesian network. *Transportation Research Part D: Transport and Environment*, *146*, Article 104845. https://doi.org/10.1016/j.trd.2025.104845

Ward, J. R., Agamennoni, G., Worrall, S., Bender, A., & Nebot, E. (2015). Extending time to collision for probabilistic reasoning in general traffic scenarios. *Transportation Research Part C: Emerging Technologies*, *51*, 66–82. https://doi.org/10.1016/j.trc.2014.11.002

WHO (2023). Global status report on road safety 2023. https://www.who.int/teams/social-determinants-of-health/safety-and-mobility/global-status-report-on-road-safety-2023

Wu, D., Xing, L., Li, Y., Wong, Y. D., Lee, J. J., & Dong, C. (2025). A framework for real-time traffic risk prediction incorporating cost-sensitive learning and dynamic thresholds. *Accident Analysis and Prevention*, *218*, Article 108087. https://doi.org/10.1016/j.aap.2025.108087

Xu, Y., Shao, W., Li, J., Yang, K., Wang, W., Huang, H., Lv, C., & Wang, H. (2022). SIND: A drone dataset at signalized intersection in China. *IEEE 25th International Conference on Intelligent Transportation Systems (ITSC)*, Macau, China, 2471–2478. https://doi.org/10.1109/ITSC55140.2022.9921959

Zhang, E., Zhang, R., & Masoud, N. (2023). Predictive trajectory planning for autonomous vehicles at intersections using reinforcement learning. *Transportation Research Part C: Emerging Technologies*, *149*, Article 104063. https://doi.org/10.1016/j.trc.2023.104063

Zhao, L., Zhou, W., Xu, S., Chen, Y., & Wang, C. (2025). Multi-agent trajectory prediction at unsignalized intersections: An improved generative adversarial network accounting for collision avoidance behaviors. *Transportation Research Part C: Emerging Technologies*, *171*, Article 104974. https://doi.org/10.1016/j.trc.2024.104974